



an ASME  
publication

\$1.00 PER COPY  
50¢ TO ASME MEMBERS

The Society shall not be responsible for statements or opinions advanced in papers or in discussion at meetings of the Society or of its Divisions or Sections, or printed in its publications.

*Discussion is printed only if the paper is published in an ASME journal.*

Released for general publication upon presentation

## Distribution of Pressure in an Opposed-Anvil, High-Pressure Cell<sup>1</sup>

H. C. DUECKER

E. R. LIPPINCOTT

Professors,  
Department of Chemistry,  
University of Maryland,  
College Park, Md.

*Apparatus*

The distribution of pressure is determined from spectral data taken from microsections of a substance with a pressure-sensitive absorption band mounted in a diamond-anvil, high-pressure cell. Since the position of the absorption band is known as a function of pressure from independent measurements, each piece of spectral data can be converted to a pressure, to develop a pressure-contour map. A derivation of the expected pressure distribution is made in terms of the compressibility of the material. The equation developed to relate the pressure,  $P$ , at some point,  $r$ , along the radius of the diamond is

$$\frac{r_0^2 - r^2}{r_0^2 - r_a^2} = \frac{aP - bP^2}{aP_a - bP_a^2}$$

where

$P_a$  is the applied pressure,  $r_a$  is the position along the radius corresponding to the applied pressure, and  $r_0$  is the radius of the diamond surface. Using further relations, we can evaluate  $r_a$  and the maximum pressure within the cell. These parameters depend on the applied pressure and the compressibility of the material. In general, the maximum pressure is about two times the applied pressure, which is realized at about  $r_a = 0.7 r_0$ . The agreement with the experimental data is very satisfactory. A method is described for determining compressibility from pressure-distribution data.

<sup>1</sup>This work was supported in part by a grant from the U. S. Army Research Office (Durham) and a Materials Science Program, Advanced Research Projects Agency, Department of Defense.

Contributed by the Research Committee on Pressure Technology for presentation at the Winter Annual Meeting, New York, N. Y., November 29-December 4, 1964, of The American Society of Mechanical Engineers. Manuscript received at ASME Headquarters, August 10, 1964.

Written discussion on this paper will be accepted up to January 10, 1965.

Copies will be available until October 1, 1965.



# Distribution of Pressure in an Opposed-Anvil, High-Pressure Cell

H. C. DUECKER

E. R. LIPPINCOTT

Optical studies under very high pressure suffer from the lack of well-standardized experimental equipment and procedures. A preliminary requirement for this standardization is an understanding of the classical fixed anvil-high pressure cell of Bridgman, since other types of cells are generally calibrated using transition pressures reported by him. The distribution of pressure within a Bridgman-type cell is of particular concern.

A Bridgman-type cell with diamond optics anvils has been described (1)<sup>1</sup> and its application to spectral (2) and optical studies (3) has been reported. The optical quality of the diamonds permits high-resolution optical observations and photography as well as spectral measurements. The fact that materials can be viewed simultaneously under a continuous range of pressures, from 1 atm to about twice the applied pressure, makes it particularly well adapted to the study of pressure-induced phase changes (4).

A substance whose spectral characteristics are known as a function of pressure may be applied to the determination of the pressure distribution within this cell if spectral data can be obtained from different microsections of the sample (5).

## HISTORICAL

Bridgman was aware of a pressure gradient (6) but he was unable to evaluate it satisfactorily so that the pressures reported in his studies are "mean applied pressures."

Bridgman gave a qualitative description of the factors leading to an uneven pressure distribution; viz., the coefficient of friction of the sample at the anvil surface, the applied pressure, the radius of the piston and the thickness of the sample film between the pistons. A quantitative description of the effect of these factors has been derived recently and will be discussed.

Perhaps, the earliest evidence indicative of a pressure gradient was the formation of a depression in the surface of the hardened-steel pistons after only a few experiments. In this regard, he was able to measure only the permanent deformation at 1 atm and not the deformation of the piston under pressure during the experiment. The measurement of this depression led him to believe that

<sup>1</sup> Underlined numbers in parentheses designate References at the end of the paper.

the pressure is greatest in the center of the piston. However, he felt that under certain conditions the portion of the piston under the highest pressure would yield, with the result that the pressure may be greater at some distance away from the center. In conclusion, he was unable to arrive at any consistent pattern with the many materials tested, and thus used average pressure values. The introduction of less deformable anvils, e.g., pyrophyllite and diamond, presumably should lead to a less complicated pressure distribution than that observed by Bridgman. Recently, there have been attempts to assess the pressure variation in opposed anvil-high pressure cells. Roy et al (7) have observed the location i.e., distance from the center, of the  $Bi_{I-II}$  transition at 25.4 kbar for various applied pressures. The somewhat limited data indicate an increase in pressure from the edge to the center such that the maximum pressure at the center is about 2.5 times the applied pressure. Christiansen et al (8) compressed silica glass in a similar type of pressure cell and have used the densification of the glass to evaluate the pressure distribution. The resulting pressure distribution is different from that reported by Roy et al, being lower in the center than at the edge. Deaton and Graf (9), using the  $Bi_{I-II}$  transition, have compared the pressures at the center, edge and face of a tetrahedral anvil-high pressure cell. While the pressure at the face and center were within a few percent of each other, pressures nearer the edge were only 70 percent of the value at the center.

A number of attempts have been made to evaluate mathematically the pressure distribution under rigid Bridgman type anvils (10-12). These derivations arrive at a relation of the form,

$$P = P_0 G(r) e^{(2f/h)(r_0 - r)}$$

where  $f$  is the coefficient of friction,  $h$  the distance between the anvils,  $P$  the pressure at radius  $r$  and  $G(r)$  is a function of  $r$ , or unity. Jackson and Waxman (12) have discussed the expected pressure distribution for elastic as well as plastic materials with different arrangements of anvil and sample. For plastic materials such as those with which we are concerned, an exponential pressure increase toward the center is predicted requiring an abrupt (and presumably objectionable) pressure rise at the center.

Thus, a need for a more precise measurement



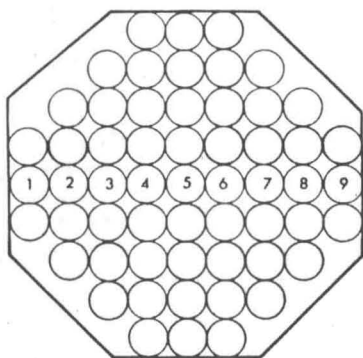


Fig. 1 Microsectioning procedure - contour

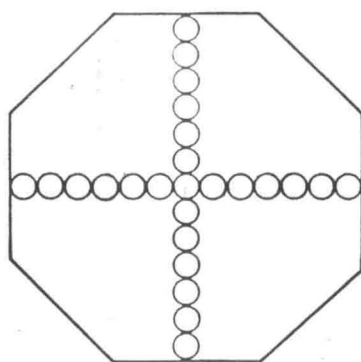


Fig. 2 Microsectioning procedure - gradient

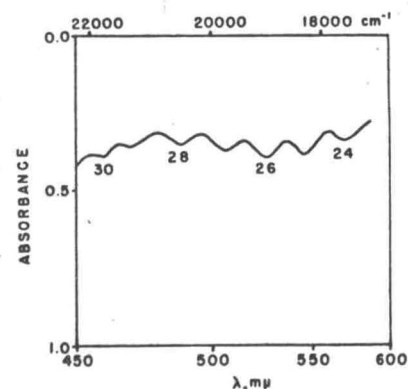


Fig. 3 Interference fringes from diamond cell

of the magnitude and especially the shape of the pressure distribution in high-pressure cells is indicated before very reliable state and spectroscopic data can be obtained using high-pressure cells with a pressure gradient.

#### EXPERIMENTAL METHODS

A microscope spectrophotometer described elsewhere (13) has been built for the determination of the spectra of selected areas of substances mounted in the diamond anvil high pressure cell. The physical dimensions of the cell make necessary the use of long-working-distance optics. Conoscopic optics normally used with the universal stage satisfy this requirement. Using these it is possible to select an area as small as  $10^{-7} \text{ cm}^2$ . The area of the diamonds used in our experiments is  $3.2 \times 10^{-3} \text{ cm}^2$ . Thus, 3000 spectral determinations would be required to completely cover the diamond area under these conditions. Since 50-100 measurements are enough to characterize properly the pressure distribution within the cell, we use scan areas of approximately  $4 \times 10^{-5} \text{ cm}^2$ . Fifty-seven such circular sectors are taken from each specimen as indicated in Fig. 1.

After it was established that the pressure distribution was symmetric about the center of properly aligned diamonds, the sampling procedure was simplified to a pair of diametric measurements, with 17 such measurements from the scheme shown in Fig. 1 or by the use of 25 microsections with reduced area as shown in Fig. 2. Care was taken to get a reasonably good alignment of the diamonds. Microsections with an air pocket were avoided, as the spectra taken from such areas were not quantitatively correct and perhaps not qualitatively accurate.

Use was made of the larger of these voids, however, since the spectral pattern obtained often

has a sufficient interference pattern that the spectral positions of the fringes could be determined. Such fringes are often observed owing to reflections from parallel plates (in this case the diamonds) (14). The order,  $N$ , of the interference fringes can be assigned from the observed frequencies since

$$N/N + 1 = \lambda_N / \lambda_{N+1}$$

The thickness,  $t$ , of the air layer (and hence the sample thickness) can then be calculated by the relation

$$t = N/2 n_D N$$

where  $n_D$  is the index of refraction of the air. This procedure could be used only when the void was sufficiently large and the conditions for interference were met. Sample thicknesses of from 8 to 15 were so measured. An example of the typical interference pattern is given in Fig. 3 along with the assigned fringe order. This pattern was obtained from a sample of nickel dimethylglyoxime diluted with 3 parts KBr at an applied pressure of 4 kbar. An attempt will be made in the future to apply the method to the measurement of sample extrusion and the determination of the deformation of the diamond anvils under pressure, although it is now doubtful that the method will be sensitive enough for the latter determination.

For pressure-distribution studies it is best to select a substance which has an absorption band which shifts with pressure. Nickel dimethylglyoxime is known to have such an absorption band at  $19,000 \text{ cm}^{-1}$  and has been shown by Zahner and Drickamer (15) to have a shift of  $-80 \text{ cm}^{-1}/\text{kbar}$ . This shift has been verified by measurements in our laboratory, by scanning the entire sample in the diamond high-pressure cell. Thus, if we determine the peak position of the absorption band for each



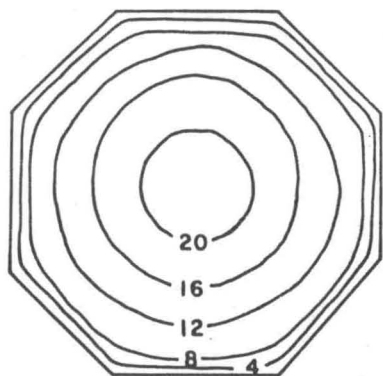


Fig.4 Pressure contours - good diamond alignment, sample of nickel dimethylglyoxime diluted with 3 parts KBr at an applied pressure of 12 kbar

microsection of a sample of nickel dimethylglyoxime in the diamond cell and know the peak position as a function of pressure, we can calculate the average pressure of each microsection. By using the microsectioning pattern of Fig.1, we can connect points of equal pressure and derive a pressure contour map such as that shown in Fig.4. A contour map from a similar sample with poorly aligned diamonds is given in Fig.5. If instead we use the microsectioning pattern shown in Fig.2, we get a pressure-distribution curve along the diameter of the cell.

Solid nickel dimethylglyoxime has an extinction coefficient of about  $3 \times 10^3 \text{ cm}^{-1}$  at  $19,000 \text{ cm}^{-1}$  so that it is difficult to get a good spectrum of the material unless great care is taken to get a particularly thin specimen. This substance was, therefore, in some experiments diluted with an alkali halide. A comparison of the spectra from diluted samples with that of the pure material indicated no spectral effects due to chemical interaction.

Aside from the spectrophotometric method, two other methods for the determination of pressure gradients have been used. A photographic method has been particularly applicable to the determination of the pressure distribution of materials with an absorption edge, such as mercurous compounds or thalious halides. In this method, the sample is viewed in the diamond cell under the microscope with monochromatic radiation. Those portions of the sample whose absorption edge is below the wavelength of radiation used will be transparent while those portions of the sample whose absorption edge is above will appear black. The boundary between the regions corresponds to the pressure at which the absorption edge occurs

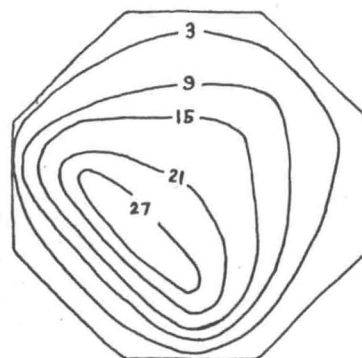


Fig.5 Pressure contours - poor diamond alignment, same sample used in Fig.4

at the illumination wavelength. Thus, if the position of the absorption edge of a substance is known as a function of pressure, a series of photographs taken at different wavelengths can be used to develop pressure contour maps in much the same way as described above.

The method of following the position of a phase transition used by Roy et al (7) and Van Valkenburg (3) is simplified by the use of photographs. In this method, however, one can only follow the position of one contour (the pressure of phase transition) as a function of applied pressure and does not obtain pressure contours like those given with the other two methods.

#### EXPERIMENTAL PROCEDURE

The procedure for a typical pressure-gradient determination of the spectrophotometric method follows. Nickel dimethylglyoxime is ground in a mortar with 2, 3 or 5 parts by weight of KBr, NaCl or LiF until the sample is uniformly mixed. A milligram of the sample is placed on the larger diamond anvil and the smaller diamond anvil is placed in the cell and the diamonds are pressed together. The pressure is increased to about 5 kbars where the diamonds may be checked for proper alignment by noting the uniformity of the color variation across the diamond surface. The pressure is reduced to room pressure and then reapplied slowly to the desired pressure. Thus, the spectral measurements were made under conditions of increasing pressure.

A complete analysis of the friction of the lever-and-piston system has not been made but it was found that the hysteresis of the pressure data from the cell could be reduced substantially by liberally lubricating the screw of the pressure cell and by working the screw back and forth a

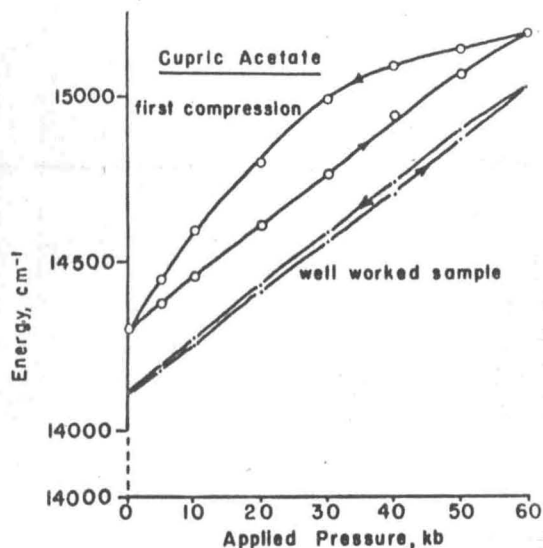


Fig. 6 Pressure hysteresis in diamond cell

fraction of a turn about the position giving the desired pressure. (This procedure probably provides somewhat the same working of the sample as the anvil in Bridgman's cell.) The reduction in the hysteresis by this method is shown in Fig. 6.

After working the sample properly in the diamond high-pressure cell, it is placed on the stage of the microscope and positioned while viewing with the stage ocular at a magnification of 125X. The sample is secured to the stage and then viewed with the microsectioning ocular (at a magnification of 180X) without the fixed aperture in position. The desired fixed aperture is slid into position and the sample image is moved with respect to the fixed aperture (with the aid of the objective centering screws) until the desired position is found. A fine adjustment on the fixed aperture slide is provided which makes this adjustment still easier. However, if one is making quantitative measurements, it is necessary to maintain the position of the fixed aperture slide so the image will be always projected onto the same position of the photocell surface. The 3-mm fixed aperture is used in the microsectioning pattern shown in Fig. 1 and the 2-mm aperture for the pattern shown in Fig. 2.

The monochromatic light source is now used to illuminate the specimen and the alignment checked again before projecting the apertured sample image directly onto the photocell for the spectral determination. The spectrophotometric scans were made from  $750\text{m}\mu$  down to  $400\text{m}\mu$  in the case of nickel dimethylglyoxime. This range is adequate to cover the red shift from  $19,000\text{ cm}^{-1}$  to  $13,500\text{ cm}^{-1}$  corresponding to pressures up to 70 kbar.

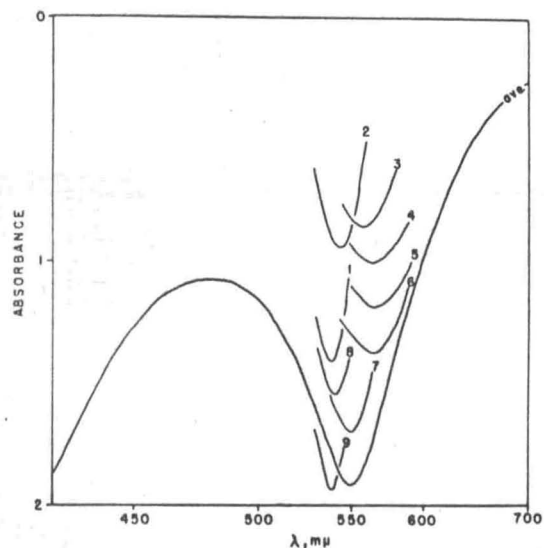


Fig. 7 Spectral data from positions along cell diameter, data taken from positions indicated in Fig. 1

A typical set of data from across one diameter of the diamond cell containing nickel dimethylglyoxime diluted with five parts of LiF is given in Fig. 7. The absorbance values are not accurate since some of the curves have been moved up or down to permit the reader to see the frequency shift with pressure.

The determination of pressure contours by the photographic method has been used with thallium bromide and nickel dimethylglyoxime. Zahner and Drickamer have reported a shift of  $-115\text{ cm}^{-1}/\text{kbar}$  for the absorption edge of TlBr (16). Polaroid high speed (ASA 3000) film was used to make photos of these substances. The monochromator of the model 350 spectrophotometer was used for the illumination. The sample preparation is the same as given above except neither of the materials were diluted. The pressure contour being obtained from each photograph. The contour lines of five to ten photographs at different wavelengths were taken for each sample under pressure.

#### EXPERIMENTAL RESULTS

Optical observation of nickel dimethylglyoxime in the diamond high-pressure cell had led to the conclusion that the pressure decreases from the center of the cell to the edge and that the incremental change in pressure increases toward the edge.

These observations were supported by the data obtained in our early studies on nickel dimethylglyoxime diluted with 3 parts KBr. Fig. 5 is a contour map of a sample at 12 kbar mounted be-



tween improperly aligned diamonds. If an average pressure value is assigned to each terrace of the contour map and multiplied by the area of the terrace, an average pressure of 11.9 kbar is obtained, in good agreement with the applied pressure. A similar determination for Fig.4, representing the same sample at 12 kbar with well aligned diamonds, gives a value of 12.3 kbar.

A similarly shaped pressure contour map was obtained for pure nickel dimethylglyoxime using the photographic method. These photographs are given in Fig.8 with the illumination used and the assigned pressures. It is much more difficult to determine the position of the boundary at higher pressures owing to the broadening and decrease in intensity of the absorption band. This problem could perhaps be reduced by the use of a high-contrast film.

The photographic method has been more adequately applied to the determination of pressure contours for a sample of pure thallium bromide. Some of these photographs are given in Fig.9 and the contour maps derived at different pressures are given in Fig.10. From these studies, it can be seen that with proper alignment of the diamonds, the samples distributed uniformly about the center of the cell. Therefore, data obtained by the simpler microsectioning pattern given in Fig.2 is just as meaningful, and the mathematics of diametric profiles are more conveniently treated.

A parabolic pressure decrease from the center to the edge of the cell, in agreement with the prediction from our optical observations, was found in every experiment. However, several common deviations often occurred; e.g., at low pressures the parabola did not always extend to the edge of the diamonds as shown by the LiF curve in Fig.14. This occurred mostly with the less compressible materials and at low pressures. It is the result of a sharper pressure drop near the edge than expected and is probably due to the orientation of the sample during the high-pressure working procedure, preceding the investigation at the low pressure. It appears that the high-pressure gradient is "frozen in" near the edge of the cell as the pressure is decreased; i.e., the rearrangement of the material near the edge is exceedingly slow under these low pressure conditions.

Another flaw in the curves is an occasional bump of too great a magnitude to be of instrumental origin. This appears to be due to the lack of a precisely uniform layer of material between the diamonds, as it too occurs with the less compressible materials. Another cause of such defects is the occasional formation of "materials streams" during the extrusion of the sample from the cell on initial compression. The subsequent fissure

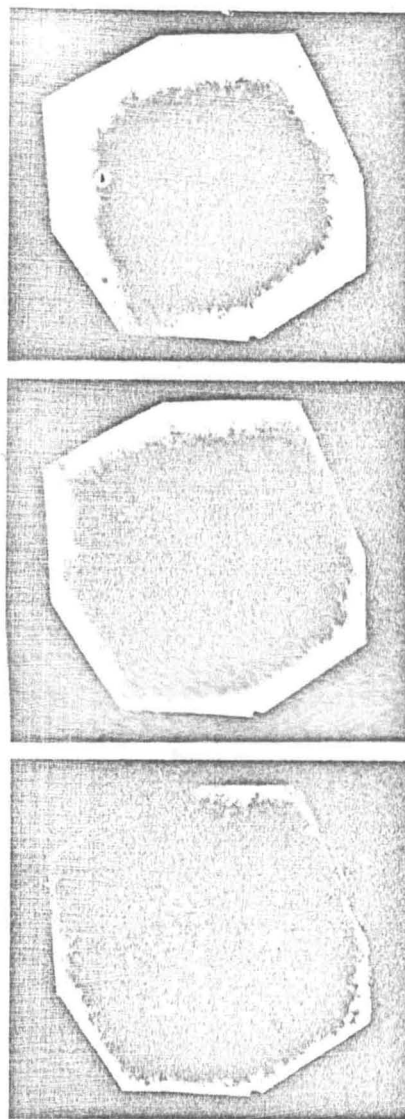


Fig. 8 Photos of Ni(DMG)<sub>2</sub> in cell taken at various wavelengths

formation within the sample prevents a completely uniform redistribution of the sample. In some cases where the materials streams are quite large, and numerous, a steeper pressure gradient is observed, simply because the lower effective contact area results in a higher average pressure.

A third problem which can be observed in some of the data reported is that of obtaining an exactly uniform distribution about the center of the diamond. At the time the measurements were made, fine adjustments of the diamond alignment were not made on each compression because we were looking for the effect of increased pressure on the alignment of the diamonds. In this regard, we learned that the diamonds have little or no "self-aligning" tendency. While this may at first appear to be a disadvantage, it is a very desirable



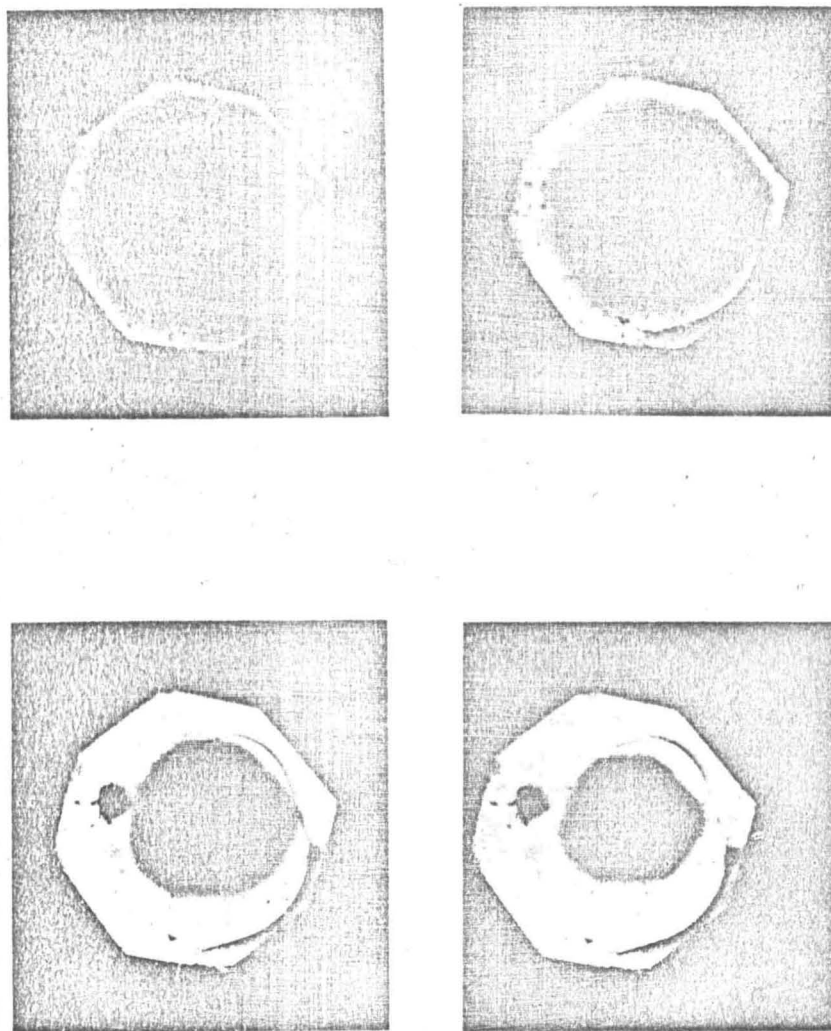


Fig. 9 Photos of TlBr in cell taken at various wavelengths

characteristic in the long run, since rather than adjust to a roughly dispersed sample placed between the diamonds, they crush and/or redistribute the sample into a thin reasonably uniform layer. (The uniformity of such a layer is probably a function of the compressibility of the sample and the area of the diamonds.)

After the qualitative observations an attempt was made to evaluate other parameters affecting the pressure distribution. The distribution across the diameter of the cell for a sample of nickel dimethylglyoxime diluted with 2 parts NaCl at different pressures is given in Fig. 11. These curves are representative of curves obtained between 10 and 60 kbar. The curves are nearly parabolic in shape, although a more critical plot, viz.,  $P$  versus  $(\Delta r)^2$ , where  $\Delta r$  is the normalized distance from the center of the diamond, is not exactly linear as expected for a true parabola. This latter type of plot representing the data in Fig. 11 is given in Fig. 12. As mentioned in the

foregoing, curves obtained at 5 kbar or less were not generally true parabolas. Pressure gradient studies in the sub-10 kbar range were not exhaustively studied, since data from the literature in the very high-pressure region (above 10 kbar) is of primary concern.

The effect of diluent concentration is demonstrated by the pressure distribution given in Fig. 13 for nickel dimethylglyoxime diluted with 2, 3 and 5 parts of NaCl as indicated. The elastic properties of nickel dimethylglyoxime are not known but from our studies, it appears to be less plastic than LiF, NaCl, KBr or TlBr and gives a less parabolic distribution in the pressure cell than these materials. In high dilutions, the mixture behaves more like NaCl and there is little resistance to forming a parabolic distribution about the center (as justified later in the discussion). As the dilution is decreased the pressure distribution becomes more nearly like that of pure nickel dimethylglyoxime. More light will be shed on the

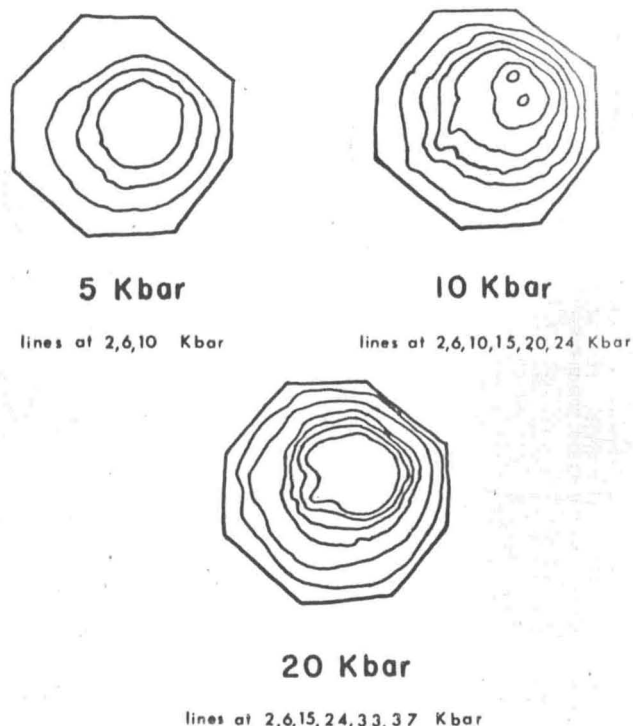


Fig. 10 Pressure contours - TlBr

solution of this problem later when compressibility data is used to derive a pressure gradient profile.

An example of the effect of the alkali halide used as a diluent is given in Fig. 14. The least compressible (and perhaps least plastic) material, LiF, gives a flatter distribution since some resistance is offered to the uniform redistribution of material in the cell, while the curve for the more compressible KBr is more nearly parabolic.

#### DISCUSSION

The empirical pressure distribution found in these studies

$$P = k (\Delta r)^2$$

is considerably different from that predicted by stress analysis, although a pressure increase toward the center is predicted in both cases.

The stress-analysis approach is limited by the complexity of the differential equations derived to include the factors known to affect the pressure distribution. In order to get solutions of these equations, assumptions or approximations must be made with respect to one or more of the variables.

It occurred to us that the pressure distri-

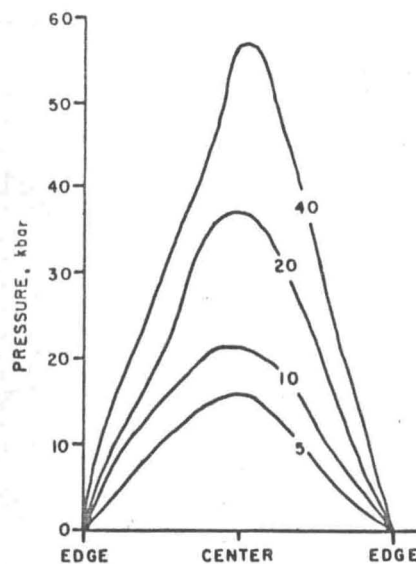


Fig. 11 Pressure gradient at 5, 10, 20 and 40 kbar

bution might be related to some experimentally determined property of the material being investigated, such as the compressibility. While these data are not available for pure nickel dimethylglyoxime, they are available for the alkali halides which we used as diluents. At diluent concentrations of 70 - 80 percent, the mixtures behave considerably different from pure nickel dimethylglyoxime and not unlike the pure alkali halide used as the diluent. Therefore, an attempt was made to determine the expected pressure distribution from compressibility data on the alkali halides.

If a pressure gradient exists within the sample wafer compressed between the diamond anvils, a compressibility gradient must also exist within the wafer, since the compressibility of a material is known to be a function of the pressure. For most materials, therefore, we would expect the material in the center of the diamond to be less compressible (although more compressed, compact or of higher density) than material nearer the edge of the diamonds which is at a lower pressure. Since the compressibility of many materials is known as a function of pressure, we should be able to determine the compressibility distribution between two known pressures. In our experiments, we know the pressure at the edge approaches 1 atm and, in addition, we have a reasonably accurate measure of the applied pressure,  $P_a$ , from the compression of the calibrated spring.

The instantaneous compressibility,  $k$ , is defined as

$$k = -1/V (\partial V / \partial P)_T$$



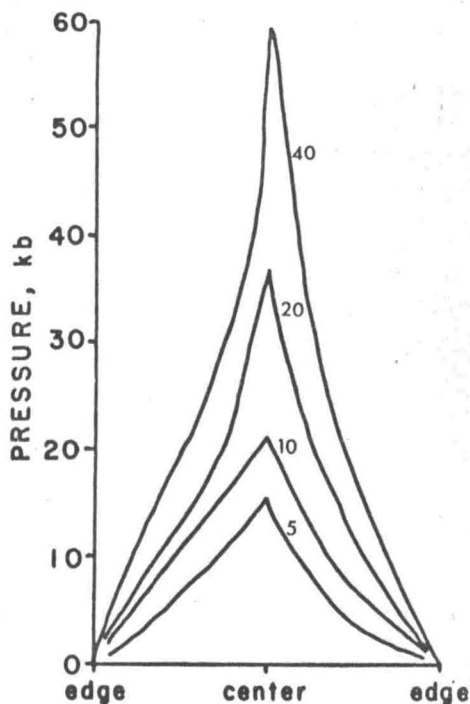


Fig. 12 Pressure versus  $(1-r^2)$  at 5, 10, 20 and 40 kbar

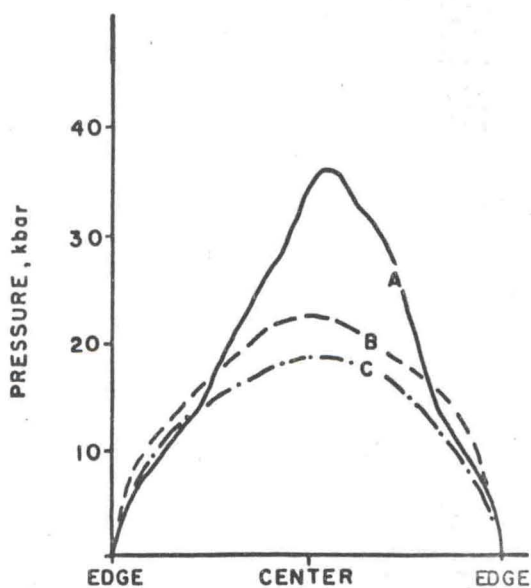


Fig. 13 Effect of diluent concentration of pressure gradient, — 5 parts NaCl by weight, - - 3 parts NaCl by weight, ··· 2 parts NaCl by weight

but at higher pressures where  $V$  becomes large it has become customary to define a compressibility,  $\beta$ , as

$$\beta = -1/V_0 \left( \frac{\partial V}{\partial P} \right)_T$$

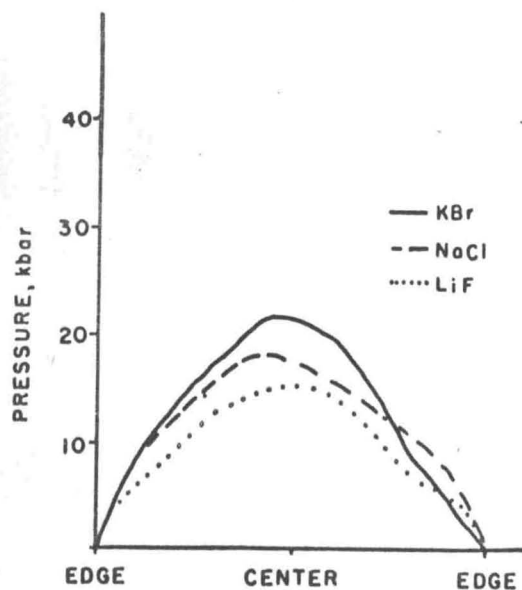


Fig. 14 Pressure gradient with different diluents, all diluents at 3 parts by weight

since the volume at 1 atm is well known and this definition lends itself more readily to an accurate experimental determination. In addition, this value is of more importance to the engineer who is particularly interested in compressibility data. Thus, the compressibilities in the literature are  $\beta$ -values, although they are often reported in the form

$$-\Delta V/V_0 = aP - bP^2 \text{ from which } \beta = a - 2bP \quad (1)$$

Values of  $\Delta V/V_0$ ,  $a$  and  $b$  are available for some representative materials at  $30^\circ$  as well as  $\Delta V/V_0$  values for some of the alkali halides at pressures from 5 to 50 kbar at  $20^\circ$ . Good compressibility data above these pressures are not available so that it is difficult to establish a good empirical relation over a very wide pressure range. At 30 to 50 kbar the  $bP$  term of relation (1) is already quite important. A theoretical treatment of compressibility based on finite-strain theory requires an even greater pressure dependence (17). Thus, the lack of good compressibility data prevents a detailed evaluation of the equations derived below at applied pressures greater than 20 kbar. (Unfortunately, experimental factors discussed earlier limit the evaluation at pressures of 10 kbar or less.)

Let us consider a confined sample in the form of a cylindrical wafer mounted between nondeformable diamond anvils with radius,  $r_0$ , separated by a distance,  $h$ , at an applied pressure,  $P_a$  (see Fig. 15). Now the volume,  $V$ , may be expressed





Fig. 15 Pressure-volume relations in diamond cell

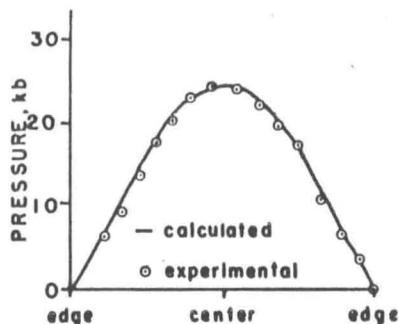


Fig. 16 Calculated pressure gradient - TlBr, 12 kbar

$$V = f(P, T, h, r) = \pi r_0^2 h$$

At constant temperature and pressure

$$\left(\frac{dV}{dP}\right)_{P, T, r} = \pi r_0^2 \left(\frac{dh}{dP}\right)_r$$

However, this is the same volume change which would occur at a given applied pressure in an identical system of constant  $h$  and variable  $r$ , Fig. 26(b), i.e.

$$\left(\frac{dV}{dP}\right)_{P, T, h} = 2\pi r h_0 \left(\frac{dr}{dP}\right)$$

This volume change can be related to  $\beta$  and give a relations for  $dP/dr$ , the pressure gradient. Combining the definition of  $\beta$ , equation (1) and the foregoing expression, we get

$$-(1/V_0) 2\pi r h_0 \left(\frac{dr}{dP}\right) = \beta$$

Multiplying both sides by  $V_0/\Delta V_a$ , where  $\Delta V_a = \pi h_0(r_0^2 - r_a^2)$ , we get

$$-(2r/r_0^2 - r_a^2) dr = (\beta dP) (V_0/\Delta V_a)$$

Integrating between  $r_0$  and  $r$  corresponding to  $P=0$  kbar at the edge to  $P=P$  at  $r$ , we get

$$-\int_{r_0}^r (2r/r_0^2 - r_a^2) dr = V_0/\Delta V_a \int_0^P \beta dP$$

or

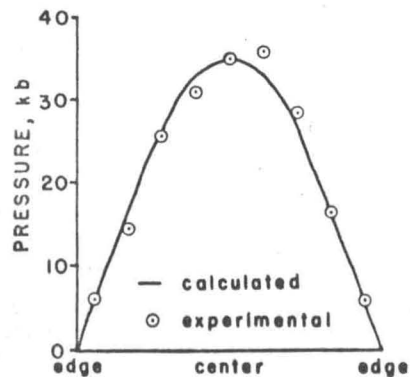


Fig. 17 Calculated pressure gradient - NaCl, 20 kbar

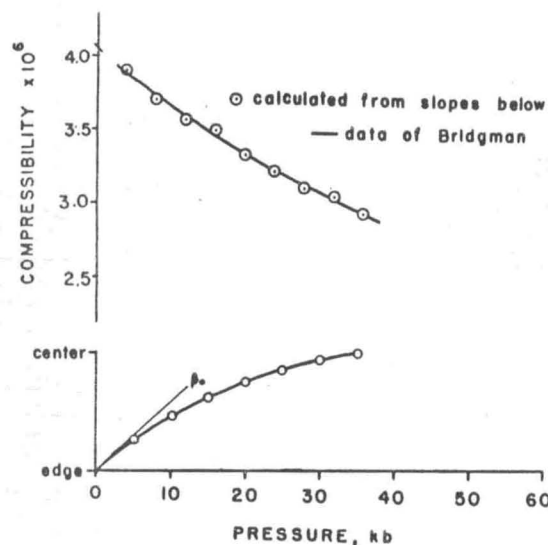


Fig. 18 Compressibility calculation - NaCl

$$\frac{1 - r^2}{1 - r_a^2} = \frac{(aP - bP^2)V_0}{V_a} = \frac{aP - bP^2}{aP_a - bP_a^2} \quad (2)$$

Similarly, the pressure,  $P$ , and  $r$  may be compared to  $P_m$ , the maximum pressure at the center of the cell by means of a similar derivation to get relation (3).

$$\frac{1 - r^2}{1 - r_m^2} = \frac{(aP - bP^2)V_0}{\Delta V_m} = \frac{aP - bP^2}{aP_m - bP_m^2} \quad (3)$$

Now it is necessary to introduce another relation to evaluate the constant  $r_a$ ; viz.

$$\bar{P} = \frac{\sum_1 A_1 P_1}{\sum_1 A_1}$$



where  $P_1$  is the pressure of any circular ring about the center and  $A_1$  is the area of the ring. Thus, the denominator is the total area of the diamond equal to  $\pi r_o^2$ .  $\bar{P}$ , the average pressure is assumed to be equal to the applied pressure,  $P_a$ , as should be the case for the frictionless system. Now as  $1 \rightarrow \infty$ , we can apply the integral over all pressures from 0 to  $P_m$ , the maximum pressure in the cell.

$$\bar{P} = \int_0^{P_m} A_1 dP / \pi r_o^2 = \int_0^{P_m} r^2 dP / r_o^2$$

We can evaluate  $r^2$  in terms of  $P$  since from relation (3)

$$r^2 = 1 - (aP - bP^2/aP_m - bP_m^2)$$

Therefore

$$\bar{P} = \int_0^{P_m} dP - (1/aP_m - bP_m^2) \left( \int_0^{P_m} aP dP - \int_0^{P_m} bP^2 dP \right)$$

$$P_a = \bar{P} = P_m - \left[ (aP_m^2/2) - bP_m^3(3) \right] (1/aP_m - bP_m^2)$$

$$\text{from which } P_a/P_m = 0.5 + 6(aP_m - bP_m^2)/bP_m^2. \quad (4)$$

From this relation  $P_m$  can be determined when the applied pressure is known. Since the  $b$  term is generally small, there is no significant effect on  $P_m$  at low pressures. For example, for sodium chloride at 10 kbar,  $P_m/P_a = 1.997$ .

Term  $r_a$  can be determined by combining expressions (2) and (3) to obtain

$$r_a^2/r_o^2 = 1 - (aP - bP^2/aP_m - bP_m^2) \quad (5)$$

The effect of  $P$  on  $r_a$  is greater than the  $P_m/P_a$  relation above, e.g., at  $P_m = 10$  kbar with sodium chloride,  $r_a = 0.692 r_o$  while at 40 kbar,  $r_a = 0.621 r_o$ .

Thus, it can be seen that at low pressures

$$\lim_{P_a \rightarrow 0} P_m/P_a = 2.0 \text{ and } \lim_{P_a \rightarrow 0} r_a/r_o = 0.707$$

The limits of these relations cannot as yet be determined at higher pressures as compressibility data above 40 kbar is not adequate. In general, therefore, this theory predicts  $P_m/P_a \leq 2.0$  and decreases with increasing pressure. Further,  $r_a \leq 0.707 r_o$  and decreases (or moves toward the center) as pressure increases.

The agreement of the experimental data with this theory is very good with regard to the general shape of the pressure distribution curve. The curves shown in Figs. 11, 13 and 14 all have less

parabolic character as the pressure increases toward the center as predicted by relation (2) and demonstrated in Fig. 12. The calculated curve for pure thallium bromide is given in Fig. 16 along with the experimental points. As indicated earlier, the diamonds were not aligned properly to get exact agreement but the shape is fairly well established. A further example using a more compressible material at a higher pressure is given in Fig. 17. This curve is taken from a sample of nickel dimethylglyoxime diluted with 2 parts sodium chloride at an applied pressure of 20 kbar. At this pressure the calculated deviation from parabolism at the center is noticeable but in quite good agreement with the data.

The relation  $P_m/P_a \leq 2.0$  is not so well verified by our experiments particularly at low applied pressures. This is probably due to the improper alignment of the diamonds and the incomplete redistribution of the material between the diamonds at low pressures as discussed earlier. At higher pressures the values are less than 2.0 as predicted by the theory, Table 1. Predicted values are not given at pressures greater than 20 kbar since adequate compressibility data are not available. At 20 kbar the experimental values from well-aligned diamonds agree quite well with the calculated value for the pure alkali halide.

A further test of the  $P_m/P_a$  relation will be pursued when compressibility data over a larger pressure range becomes available at 25 deg. This may require a modification of equation (4) to include a greater pressure dependence.

Experimental and calculated values of  $r_a$  are given in Table 2 for different materials at 20 kbar, as well as some experimental values at 40 kbar. The agreement is about the same as that for the  $P_m/P_a$  relation. Thus, relation (2) adequately describes the pressure distribution of these substances in the diamond high pressure cell if distributed uniformly between properly aligned diamonds.

#### CALCULATION OF COMPRESSIBILITY FROM PRESSURE-DISTRIBUTION DATA

Compressibility data have been applied quite satisfactorily to the determination of the pressure distribution in the diamond-anvil high-pressure cell. The fact that the main barrier to giving the theory a rigorous test is the lack of adequate compressibility data suggests that the pressure gradient within the cell be applied to the determination of compressibilities. The method requires a reference compressibility much the same as the pressure distribution required a reference to the applied or maximum pressure. However, 1



TABLE 1

AGREEMENT OF EXPERIMENTAL AND CALCULATED PARAMETERS  
IN PRESSURE DISTRIBUTION ANALYSIS

Sample	$P_m/P_a$		
	20 kbar		40 kbar
	exper.	calc.*	exper.
Pure Ni(DMG) <sub>2</sub>	2.0		
Pure TiBr	2.0	1.96	
Ni(DMG) <sub>2</sub> in KBr(1:2)**	1.85	1.90	
Ni(DMG) <sub>2</sub> in NaCl(1:2)	1.80	1.95	1.43
Ni(DMG) <sub>2</sub> in NaCl(1:3)	2.0	1.95	
Ni(DMG) <sub>2</sub> in NaCl(1:3) poor alignment	1.60	1.95	

TABLE 2

Sample	$r_a/r_o$		
	20 kbar		40 kbar
	exper.	calc.*	exper.
Pure Ni(DMG) <sub>2</sub>	0.70		
Pure TiBr	0.68	0.61	
Ni(DMG) <sub>2</sub> in KBr(1:2)	0.52	0.60	
Ni(DMG) <sub>2</sub> in NaCl(1:2)	0.69	0.62	0.55
Ni(DMG) <sub>2</sub> in NaCl(1:3)	0.62	0.62	
Ni(DMG) <sub>2</sub> in NaCl(1:3) poor alignment	0.70	0.62	

\* calculation based on the pure alkali halide

\*\*phase transition at 18 kbar with a 10% volume decrease makes calculation difficult and causes a steeper pressure gradient

will be seen that the reference compressibility can be chosen as the compressibility at atmospheric pressure, a value which can be more accurately determined than perhaps at any other pressure and by independent methods.

It has been shown earlier that

$$-2r \, dr/dP = \beta / (\Delta V_a/V_o) = d(1 - r^2)/dP \quad (6)$$

In Fig. 18 it was seen that a plot of  $1-r^2$  versus pressure is not linear. Equation (6) requires nonlinearity since  $\beta$  is pressure dependent. Now, as the pressure approaches 1 atm (at the edge of the cell)  $\beta \rightarrow \beta_o$ , the compressibility at 1 atm.

Let us consider a plot, similar to that in Fig. 18 but with pressure on the abscissa since  $\beta$  is dependent on pressure. This is an experimental pressure gradient determined on a sample of nickel dimethylglyoxime diluted with 2 parts sodium chloride at 20 kbar applied pressure.  $\beta_o$  for sodium chloride is known to be  $4.1 \times 10^{-6}$  at 20°. The slope of the experimental plot at the origin was found to be  $1/17050 = 0.00586$ , so that

a ( $V_a/V_o$ ) value of 0.070 is required to give

$$\beta_o = [d(1 - r^2)/dP]_{o, \text{exper}} [\Delta V_a/V_o] \quad (7)$$

$$\beta_o = 4.1 \times 10^{-6}$$

This value of  $\Delta V_a/V_o$  is then used to convert the slopes at other points along the curve to  $\beta$ -values, since relation (7) is applicable at any pressure as well as at 1 atm. The points so calculated from the slopes are indicated in the upper part of the figure. The solid line is a plot of compressibility of pure sodium chloride calculated from  $\Delta V/V_o$  data of Bridgman (18). The agreement is surprisingly good but one must remember that  $\beta$  does not change as rapidly with pressure as  $\Delta V/V_o$  and the experimental points cannot be determined very accurately from the slopes.

The agreement with the literature compressibility values is apparently real since the pressure gradient curve for the same sample at 40 kbar gives similar results although the spread is greater, due perhaps to a less accurately known pressure profile. (These particular radial profiles were determined from only 6 experimental measurements; more points are usually required to get smooth profiles.)

Although the method appears to work fairly well, some concern should be shown about a number of problems. We would not, off hand, expect a matrix with 1 part nickel dimethylglyoxime and 2 parts sodium chloride to have exactly the same compressibility as sodium chloride. On this basis, the agreement would appear to be fortuitous. On the other hand, it appears, from qualitative observations made in this laboratory over a period of a year or two, that when a substance is diluted with 30 percent or more of a less compressible material the matrix behaves much the same as the less compressible material alone. It is rather difficult to imagine that the compressibility would not be affected by a minor component concentration of 33 percent. This is an interesting problem which must be solved before further quantitative work can be done.

The determination of slopes from a curve is neither convenient nor very accurate. If this work is continued, a large number of experimental points should be taken along the radius of near-perfectly aligned diamonds in order to obtain a smooth radial profile. A computer should be used to calculate the best curve using the best known compressibility-pressure relation. The computer should be instructed to evaluate the experimental slope at 1 atm and from a given value of  $\beta_o$ , com-

pute the compressibility at any pressure from 1 atm to  $P_m$ , the maximum pressure in the cell under the conditions used. If compressibility data is desired over a wider pressure range, the applied pressure may simply be increased appropriately and another pressure profile determined experimentally.

Although considerably more work (particularly theoretical) must be done, pressure profiles appear to offer a unique and convenient method for the determination of compressibilities. In the latter regard, compressibilities can be determined over a wide pressure range (probably up to 200 kbar) and perhaps in a single experiment. A diamond-anvil high-pressure cell equipped with a temperature jacket would probably permit the determination of compressibilities as a function of temperature as well, with only perhaps a microgram of material in a single compression, providing care is taken to obtain equilibrium conditions.

#### REFERENCES

- 1 C. E. Weir, A. VanValkenburg, E. R. Lippincott, "Optical Studies at High Pressures Using Diamond Anvils," *Modern Very High Pressure Techniques*, Butterworths, Inc., Washington, D. C., 1962, pp. 51-69.
- 2 C. E. Weir, E. R. Lippincott, A. Van Valkenburg, E. N. Bunting, "Infrared Studies in the 1 to 15 micron Region at 30,000 Atmospheres," *Journal of Research, National Bureau of Standards*, vol. 63A, 1959, pp. 55-62.
- 3 A. VanValkenburg, "High Pressure Microscopy," *High Pressure Measurement*, Butterworths, Inc., Washington, D. C., 1963, pp. 87-94.
- 4 A. VanValkenburg, "High Pressure Microscopy of the Silver and Cuprous Halides," *Journal of Research, National Bureau of Standards*, vol. 68A, 1964, pp. 97-103.
- 5 E. R. Lippincott and H. C. Duecker, "Measurement of Pressure Distribution in Fixed Anvil High Pressure Cells," *Science*, vol. 144, 1964, pp. 1119-1121.
- 6 P. W. Bridgman, "Shearing Phenomena at High Pressures, Particularly in Inorganic Compounds," *Proceedings American Academy of Arts and Sciences*, vol. 71, 1937, pp. 387-460.
- 7 M. B. Myers, F. Dacheille, R. Roy, "Pressure Multiplication Effect in Opposed-Anvil Configurations," *Review of Scientific Instruments*, vol. 34, 1963, pp. 401-402.
- 8 E. B. Christiansen, S. S. Kistler, W. B. Gogarty, "Irreversible Compressibility of Silica Glass as a means of Determining the Distribution of Force in High Pressure Cells," *Journal of American Ceramic Society*, vol. 45, 1962, pp. 172-177.
- 9 B. C. Deaton and R. B. Graf, "Pressure Distribution and Hysteresis Effects in a Tetrahedral Anvil Device," *Review of Scientific Instruments*, vol. 34, 1963, pp. 45-47.
- 10 R. Hill, "Plasticity," Oxford Press, London, 1956, pp. 50-127.
- 11 J. C. Jamieson and A. W. Lawson, "X-Ray Diffraction Studies in the 100 Kilobar Pressure Range," *Journal of Applied Physics*, vol. 33, 1962, pp. 776-780.
- 12 J. W. Jackson and M. Waxman, "An Analysis of Pressure and Stress Distribution Under Rigid Bridgman-Type Anvils," *High Pressure Measurement*, Butterworths, Inc., Washington, D. C., 1963, pp. 39-58.
- 13 H. C. Duecker and E. R. Lippincott, "Assembly and Performance of a Double-Beam Microscope Spectrophotometer from Commercial Instruments," *Review of Scientific Instruments*, vol. 35, 1964, September issue.
- 14 R. P. Bauman, "Absorption Spectroscopy," Wiley & Sons, New York, 1962, pp. 84-87.
- 15 J. C. Zahner and H. G. Drickamer, "Pressure Effects in Nickel Dimethylglyoxime and Related Chelates," *Journal of Chem. Phys.*, vol. 33, 1960, pp. 1625-1628.
- 16 J. C. Zahner and H. G. Drickamer, "The Effect of Pressure on the Absorption Edge in Heavy Metal Halides," *Phys. and Chem. Solids*, vol. 11, 1959, pp. 92-95.
- 17 F. D. Murnaghan, "Finite Deformation of an Elastic Solid," Wiley and Sons, New York, 1939.
- 18 P. W. Bridgman, "The Compression of 46 Substances to 50,000 Kg/cm<sup>2</sup>," *Proceedings of the American Academy of Arts and Sciences*, vol. 74, 1940, pp. 21-51.